CFD ANALYSIS OF CHEMICAL TRANSPORT IN HUMAN NOSE

M.V.SHYLA[1] and K.B. NAIDU[2]
Department of Mathematics, Sathyabama University,
Chennai-600 119, Tamil Nadu, India
[1] shylamv@yahoo.com and [2]kbnaidu999@gmail.com

Abstract

The paper aims to simulate the chemical transport of ammonia vapor with density ρ = 0.6894 kg/m^3 and coefficient of viscosity μ = 1.015e-05 kg/m-s inside the healthy Indian nose by computational fluid dynamics (CFD) technique and to analyze the olfactory sensitivity. The computed tomographic images of a healthy adult with normal nasal structure and function was used to built a physically realistic model with the help of Mimics software. Navier-Stokes and continuity equations were solved numerically for steady and unsteady state conditions by finite volume method to determine laminar flow patterns. CFD simulation was performed using Gambit and Fluent software to visualize implications for olfaction. The graphs indicate that only part of the inspired chemical passes through the olfactory airway. The total olfactory uptake for the odorant increased as inlet velocity increased.

Key words: CFD technique, CFD simulation, chemical transport, human nose.

1. Introduction

There are many benefits in CFD analysis. It is much cheaper and faster to perform CFD simulation than to conduct an experiment. CFD results can be analyzed easily . A detailed description of the flow behavior taking place at any location within the flow can be observed, thereby the effect of geometry on the flow behavior can be studied. Hence CFD analysis is performed as an alternate method to physical experiments.

Until the development of CFD analysis, the effect of sniffing on nasal airflow was very difficult to analyze. Kai Zhao et al.[1] used a CFD approach to study the effects of sniffing on nasal airflow and odorant transport. But more importance was given to analysis of nasal airflow with turburlence model. In the study done by Ishikawa et al.[2], analysis was done with unsteady model with discussion on velocity and vorticity. Subramaniam et al. [3]and Elad et al. [4]conducted similar CFD analysis but their studies did not compare airflow patterns on both sides of the nasal cavity.

In this study, a healthy Indian nose with normal function and geometry is considered for CFD analysis. Detailed velocity profile, iteration plots, pressure distribution and streamline patterns for two dimensional chemical transport of ammonia vapour inside both sides of human nasal cavity are presented. Implications of olfaction is well understood and visualized in this study.

The paper is organized as follows. Section 2 touches upon the governing differential equations, assumptions and boundary conditions. Section 3 exposes the methodology in detail. Section 4 presents our relevant discussion. Concluding remarks are drawn in Section 5.

2. Methods

2.1. GOVERNING DIFFERENTIAL EQUATION:

Navier Stokes system of equations for a two dimensional, viscous, incompressible flow

$$\nabla . \bar{q} = 0$$

$$\rho\left(\frac{\partial \vec{q}}{\partial t} + \vec{q}.\nabla\vec{q}\right) = -\nabla p + \mu\nabla^2\vec{q} \quad (1)$$

$\vec{q} = u\vec{\imath} + v\vec{j}$ is the velocity vector where u and v are the velocity components in the x & y directions respectively, p is pressure, ρ is density, and μ is viscosity.

2.2. *Boundary Conditions*

A two dimensional , laminar, chemical transport of ammonia vapor inside the human nose for steady and unsteady conditions are considered. A velocity of 0.4m/s and 0.5m/s is applied at the inlet. The walls are considered to be rigid. No slip boundary condition is assumed(velocity is zero at the boundary). The air pressure is kept at 101325 pascals on both sides of the nose. The density ρ = 0.6894 kg/m^3 and coefficient of viscosity μ = 1.015e-05 kg/m-s of ammonia vapor is taken for analysis.

3. *Methodology*

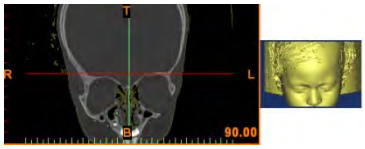

Fig.1 CT image of coronal view and 3D generated by MIMICS

The nasal model was constructed from the CT scan in dicom format using Mimics 10 software. The coronal view namely the xz view best illustrated the nasal structure. The geometry of coronal view is taken and meshed in Gambit software . The left side with 11059 nodes and 10478 quadrilateral cells. The right side with 10141 nodes and 9575 quadrilateral cells. Inlet, outlet and the wall is defined after which the 2D mesh is exported to Fluent software for analysis. The governing differential equations namely the continuity equation and Navier-Stokes equations in the integral form is solved iteratively by a segregated solver using Finite volume method in FLUENT v.6.3.26 (ANSYS. Inc.) . The solution gives a clear picture of velocity, pressure, and streamline pattern. The convergence is checked correct to 3 decimal places.

4. Results

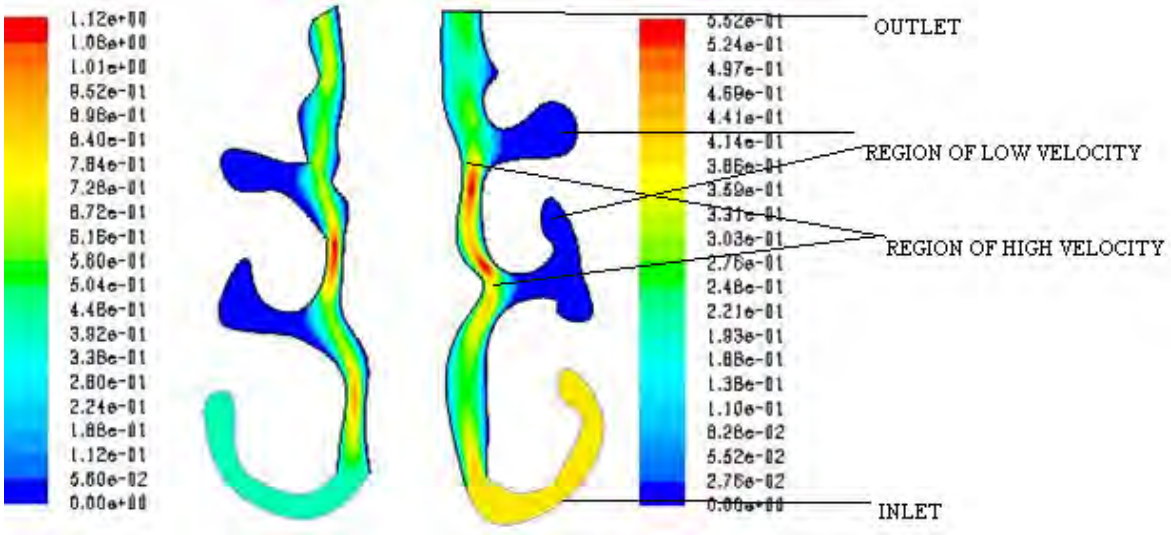

Fig 2. Contours of Velocity Magnitude(m/s) with inlet velocity 0.4 m/s

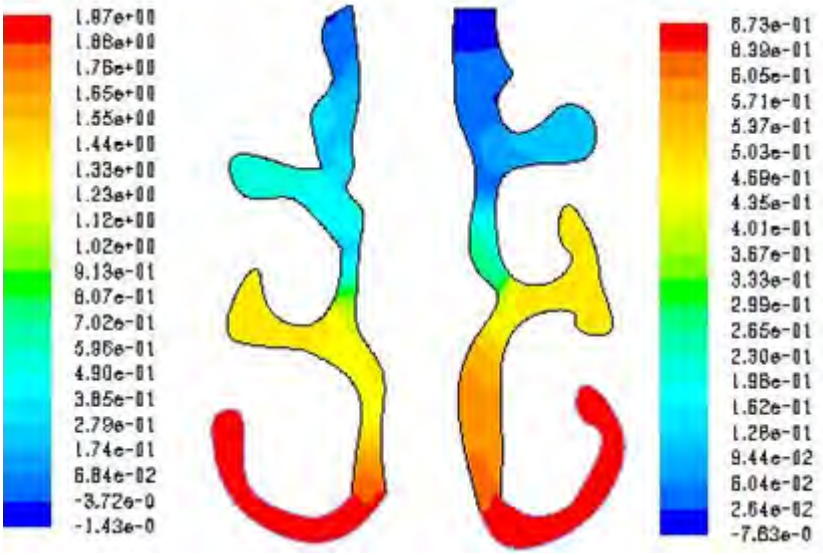

Fig 3. Contours of static pressure(pascal) with inlet velocity 0.4 m/s

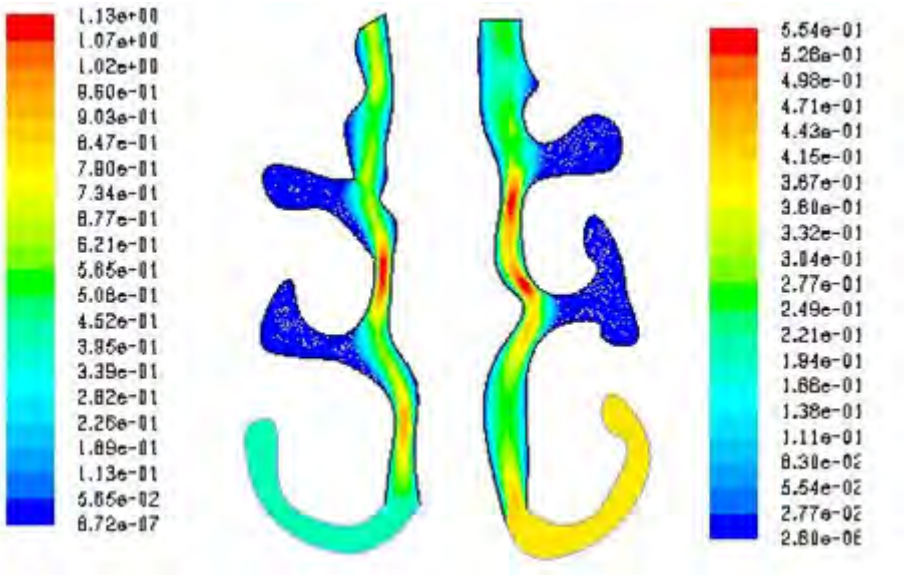

Fig 4. Streamline pattern for inlet velocity 0.4 m/s

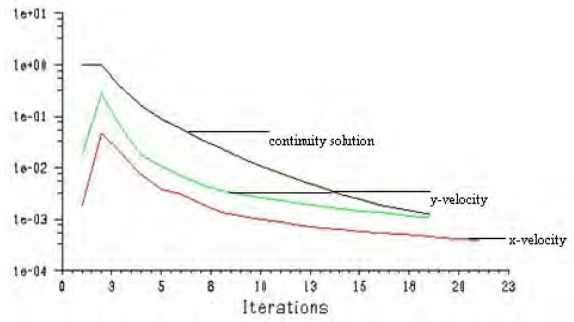

Fig 5. Iteration plot for left nasal cavity with inlet velocity 0.4 m/s

For a physically correct human nasal cavity, the left and the right sides differ in geometry [5]. Numerical studies show that highest velocities of flow appear in the middle of airway and low flows in nasal meatuses. Only part of the inspired chemical flows through the nasal cavity and reaches the olfactory region[1][6] as shown in fig2. The velocity at different points of the nasal cavity can also be viewed. Different values are identified by different colours. The lowest value by blue and highest value region is coloured red. From fig 3, pressure distribution at different points of left and right sides can be seen. The convergence of the results correct to 3 decimal places are checked as depicted in iteration plots in fig.5. The solution of continuity and Navier Stokes equation at every time step for 100 iterations is presented. The solution converges in the 21st iteration for the left nasal cavity whereas the solution converges at the 50th iteration for the right side. The streamline pattern in fig 4 clearly reveals the chemical flow through the nasal cavity to the olfactory slit in the direction of velocity and hence the implication for olfaction. There is no noticeable difference between steady and unsteady model so the flow is considered to be quasi-steady under these conditions. Increase in inlet velocity from 0.4 to 0.5 resulted in an increase in total olfactory uptake for the odorant.(3)

Table 1. Velocity and Pressure data for left and right nasal cavity for different inlet velocity

Inlet velocity	**Left**		**Right**	
	Velocity in (m/s) Olfactory slit	**Pressure in(Pa) Olfactory slit**	**Velocity in (m/s) Olfactory slit**	**Pressure in pascal(Pa) Olfactory slit**
0.4m/s	**0.153**	**-0.0075**	**0.33**	**-0.0143**
0.5 m/s	**0.23**	**-0.012**	**0.43**	**-0.15**

Conclusion

The analysis of graphs, vector plots and contours reveal that our results are consistent with those found in the literature.High velocity is observed at the middle region. Velocity is very low near the walls because of no slip condition. Only a fraction of the inspired chemical reaches the olfactory region. The structure of nasal cavity contributes to this factor in order to protect the human health from the risk of inhaled materials to a great extent.

Acknowledgement

We thank Bharat Scans, Chennai for providing us with the data, CT scan images. We are thankful to Mr. G. Vasanth Kumar, Aeronautical Department of Engineering, Sathyabama University, for providing necessary practical guidance in the preparation of this paper. We also thank Dr. B.S.M. Augustine, Head, Department of Aeronautical Engineering, for proving us the necessary hardware facilities.

REFERENCES:

[1] Zhao K, Scherer PW, Hajiloo SA, Dalton P. Effect of anatomy on human nasal airflow and odorant transport patterns. Chem Senses 2004; 29(5): 365-379.

[2] Ishikawa, Shigeru, Visualization of flow resistance in Physiological nasal respiration. Analysis of Velocity and Vorticities using Numerical Simulation(November 2006) Arch Otolaryngol Head Neck Surg, 132, 1203-1209.

[3] Subramaniam R.P., Richardson R.B., Morgan K.T., Kimbell J.S. and Guilmette R.A., Computational Fluid Dynamics Simulations of Inspiratory Airflow in the Human Nose and Nasopharynx, *Inhal. Toxicol*., **10**,1998,91–120.

[4] Elad D, Liebental R, Wening B L, Einav S. Analysis of air flow patterns in the human nose. Med and Biol Eng and Comput 1993; 31:585- 592.

[5] J.Wen 1, K.Inthavong1, Z.F.Tian1, J.Y.Tu1, C.L.Xue2 and C.G.Li2 Airflow Patterns in Both Sides of a Realistic Human Nasal Cavity for Laminar and Turbulent Conditions, "16th Australian Fluid Mechanics Conference, Crown Plaza, Gold Coast, Australia, 2-7 December 2007, pp. 68-74.

[6] Kelly J.T., Prasad A.k., and Wexler A.S., Detailed Flow Patterns in the Nasal Cavity, *J Appl. Physiol*., **89**, 2000,323-337.